Research Square

Preprints are preliminary reports that have not undergone peer review.
They should not be considered conclusive, used to inform clinical practice,
or referenced by the media as validated information.

Integrating Obesity-Susceptibility and Organokine-Related Genetic Variants Across Multiple Adiposity Phenotypes in Adults with Overweight or Obesity

Austėja Letukienė

austeja.letukiene@mf.vu.lt

Vilnius University

Valentina Ginevičienė

Vilnius University

Research Article

Keywords: obesity, overweight, genotype, phenotype, GWAS, genome-wide association study

Posted Date: November 23rd, 2026

DOI: https://doi.org/10.21203/rs.3.rs-11521683/v1

License: This work is licensed under a Creative Commons Attribution 4.0 International License.
Read Full License

Additional Declarations: No competing interests reported.

Integrating Obesity-Susceptibility and Organokine-Related Genetic Variants Across Multiple Adiposity Phenotypes in Adults with Overweight or Obesity

Austėja Letukienė[1], Valentina Ginevičienė[1]

[1] Vilnius university, Vilnius, Lithuania

Primary corrresponding author Austėja Letukienė: austeja.letukiene@mf.vu.lt

ABSTRACT

Background. Obesity is a heterogeneous condition encompassing multiple dimensions of adiposity, including overall body mass, fat distribution, and body composition. While numerous obesity-susceptibility genetic loci have been identified, less is known about the contribution of genetic variation in organokine-related pathways to different adiposity phenotypes. This study aimed to characterize the association patterns of literature-derived obesity-susceptibility and organokine-pathway genetic variants across five adiposity-related phenotypes and to determine whether these variants exhibit phenotype-specific or broader pleiotropic effects in metabolically healthy adults with overweight or obesity.

Results. A total of 133 metabolically healthy Lithuanian adults with overweight or obesity were included. Anthropometric and body composition phenotypes comprised body mass index (BMI), body weight, visceral fat percentage, waist-to-hip ratio (WHR), and total body fat percentage. Following genotype quality control, genome-wide association analyses were performed for each phenotype. Results were subsequently integrated with literature-derived obesity-susceptibility and organokine-pathway candidate variants. Associations were evaluated using additive genetic models adjusted for age and sex. False discovery rate (FDR) correction, minor allele frequency filtering (MAF $\geq$ 0.05), and linkage disequilibrium assessment were applied.

Distinct phenotype-specific association patterns were observed across adiposity measures. *IL6* variants were predominantly associated with overall body mass phenotypes (BMI and body weight), including the only association that remained significant after FDR correction (rs2069845 and rs1800795 for body weight; FDR q = 0.046). In contrast, *FTO* and *LDHA* variants preferentially associated with fat distribution and body-composition phenotypes, particularly visceral fat percentage and WHR. Variants within *POMC* and *SPARC* were specifically associated with total body fat percentage. Organokine-pathway variants showed a numerically higher proportion of broad or pan-adiposity associations than classical obesity-susceptibility variants, although the difference was not statistically significant (Fisher's exact test, p = 0.390).

Conclusions. Genetic associations with adiposity are phenotype-dependent and support the existence of partially distinct genetic architectures underlying overall body mass, fat distribution, and body composition. Evaluation of multiple adiposity phenotypes revealed biologically distinct genetic signals that would not have been identified using BMI alone. The findings further suggest a potential contribution of organokine-related pathways to obesity heterogeneity and highlight *LDHA* as a novel candidate locus warranting independent replication and functional investigation.

Keywords: obesity; overweight; genotype; phenotype; GWAS; genome-wide association study.

BACKGROUND

Obesity is a multidimensional phenotype encompassing distinct biological processes, including overall adiposity (body mass index (BMI) and body weight), fat distribution (waist-to-hip ratio (WHR)), and body composition (visceral and total fat percentage). Body fat distribution, particularly visceral adiposity, is more strongly associated with cardiometabolic risk than overall body mass, suggesting that a genetic analysis restricted to BMI may fail to capture clinically important dimensions of obesity. This distinction is well supported by epidemiological and genetic evidence. Measures of fat distribution, such as WHR and visceral adipose tissue, are correlated with BMI yet reflect different biological domains, namely regional fat deposition versus overall fat mass. Importantly, fat distribution provides cardiometabolic risk information independent of BMI [1-3]. When adjusted for BMI, visceral fat remains independently associated with increased of type 2 diabetes and coronary artery disease risk, whereas gluteofemoral fat is protective [3,4]. Similarly, genetically instrumented gluteofemoral fat, independent of BMI, has been associated with a favorable cardiometabolic profile characterized by lower LDL, cholesterol, triglycerides, and blood pressure [4].

Additional evidence supports the biological distinction between adiposity phenotypes. In obese women, visceral adipose tissue remains strongly associated with cardiometabolic risk after adjustment for total body fat, whereas abdominal subcutaneous fat does not [5]. WHR closely reflects the balance between visceral and subcutaneous fat depots in adults, whereas BMI alone cannot distinguish between these fat distribution patterns [6]. Consequently, individuals with similar BMI may exhibit markedly different body fat distribution and metabolic profiles [2, 7]. Furthermore, higher trunk fat percentage is associated with a metabolically unhealthy status even after BMI adjustment, whereas increased leg and arm fat are associated with a more favorable metabolic profile [8, 9]. Together, these observations

suggest that overall body mass, fat distribution, and body composition represent related but biologically distinct dimensions of adiposity.

Molecular pathways also differentiate obesity phenotypes. Adipose tissue, skeletal muscle, liver, and other metabolically active organs secrete signaling molecules collectively termed organokines, including adipokines, myokines, and hepatokines. These molecules regulate energy homeostasis, glucose and lipid metabolism, insulin sensitivity, inflammation, and tissue adaptation through endocrine, paracrine, and autocrine signaling mechanisms [10-16]. Altered organokine profiles have been linked to obesity, insulin resistance, and cardiometabolic disease, suggesting that organokine-related pathways may contribute to inter-individual differences in adiposity and metabolic health [11]. Importantly, several organokines, including IL-6 and fetuin-A, exert context-dependent effects that may be either protective or detrimental depending on tissue type, receptor profile, and physiological state [17]. Consistent with this complexity, metabolically healthy obesity has been associated with a more favorable organokine profile than metabolically unhealthy obesity, including higher circulating concentrations of organokines such as nesfatin-1 and neuregulin-4 [18]. Despite growing interest in organokine biology, genetic variation within organokine-related pathways has rarely been investigated alongside classical obesity-susceptibility loci within a unified analytical framework.

Most genome-wide association studies (GWAS) of obesity have focused predominantly on BMI, potentially obscuring phenotype-specific genetic effects related to fat distribution, body composition [19, 21, 22]. Although hundreds of obesity-associated loci have been identified, previous studies have generally examined genetic determinants of anthropometric traits separately from genetic variation in organokine-related pathways. This separation limits direct comparison of their relative contributions to different adiposity dimensions. Furthermore, there is increasing recognition that single-trait GWAS may overlook phenotypic

heterogeneity and dilute subtype-specific genetic signals. Recent multivariate approaches integrating BMI with waist-related measures, visceral adiposity, liver fat content, and body fat percentage have identified additional loci and adiposity subtypes beyond those detected by conventional BMI-based analyses, highlighting the value of multidimensional obesity phenotyping [21].

Despite these advances, the integration of organokine-related genetic variation into obesity characterization has lagged behind progress in body composition phenotyping and genetic subtyping. Although BMI, WHR, body fat percentage, visceral fat, and other adiposity-related traits have each been extensively investigated, few studies have evaluated these phenotypes together while simultaneously considering genetic variation in both classical obesity-susceptibility loci and organokine-related pathways.

Therefore, this study combined detailed adiposity phenotyping with genome-wide association analyses and targeted evaluation of literature-derived obesity-susceptibility and organokine-associated genetic variants in a cohort of metabolically healthy Lithuanian adults with overweight or obesity. We hypothesized that these variants would exhibit heterogeneous, phenotype-specific patterns of association rather than uniform effects across all adiposity measures, consistent with evidence that overall body mass, fat distribution, and body composition are influenced by partially distinct biological pathways. We further hypothesized that organokine-related variants would demonstrate broader associations across multiple adiposity phenotypes than classical obesity-susceptibility variants, reflecting their proposed role in systemic endocrine signalling and inter-organ communication. Accordingly, the primary aim of this study was to characterize the association patterns of literature-derived obesity- and organokine-associated genetic variants across five adiposity-related phenotypes and to determine whether these variants exhibit phenotype-specific or broader pleiotropic effects, thereby providing insight into their potential roles in the genetic architecture of adiposity.

METHODS

Study Participants and Ethical Approval

This study was approved by the Vilnius Regional Biomedical Research Ethics Committee (Approval No. 2021/11-1393-866) and conducted in accordance with the ethical principles of the Declaration of Helsinki. All participants provided written informed consent prior to enrolment.

Participants were recruited in 2025 from the Vilnius region (Lithuania) through community advertisements as part of a larger descriptive project involving adults with overweight or obesity. For the present analysis, 148 adults (94 women and 54 men; BMI > 25 kg/m², aged 25-55 years) who met criteria for metabolically healthy obesity (defined as obesity without typical cardiometabolic abnormalities) were included. All participants were able and willing to complete the study assessments. Exclusion criteria included symptomatic cardiopulmonary disease, severe kidney, thyroid, or hepatic disorders, cognitive impairment, or any condition that could compromise safe participation or adherence to study procedures. To ensure the recruitment of a metabolically healthy cohort, individuals presenting with three or more diagnostic components of metabolic syndrome, according to the National Cholesterol Education Program Adult Treatment Panel III (NCEP ATP III) criteria, were excluded. All participants underwent comprehensive phenotypic assessment and whole-genome genotyping. The present research is based on cross-sectional genotypic and phenotypic data collected at a single baseline visit.

Phenotypic Data

Five adiposity-related phenotypes were assessed during the same baseline visit at which blood samples were collected for DNA extraction and subsequent genotyping: BMI (kg/m²), body weight (kg), visceral fat percentage (%), waist-to-hip ratio (WHR), and total body fat

percentage (%). All measurements were obtained using a calibrated multi-frequency bioelectrical impedance analyser (ACCUNIQ BC300, Jawon Medical Co., Ltd., Gyeongsan, South Korea). Participants were measured barefoot and wearing light clothing, following standardized procedures, including maintenance of an upright standing posture and appropriate electrode contact in accordance with the manufacturer's guidelines. Age and biological sex were included as covariates in all association analyses. Of the 148 adults initially enrolled, six were excluded because they did not meet the inclusion criteria, leaving 142 participants who were genotyped and passed genotype-level quality control. Among these individuals, nine were excluded from subsequent analyses due to incomplete anthropometric data (6.3 % missing), resulting in a final analytical sample of 133 metabolically healthy adults with overweight or obesity and complete phenotypic data for phenotype-specific genome-wide association analysis. The normality of continuous variables was assessed using the Shapiro-Wilk test. Variables that deviated significantly from a normal distribution ($p < 0.05$) are presented as median and interquartile range (IQR), whereas normally distributed variables are presented as mean and standard deviation (± SD).

Candidate Variant Selection

To evaluate whether genetic variants previously implicated in obesity susceptibility and organokine-related pathways were associated with adiposity phenotypes in the present cohort, a non-redundant candidate variant panel was assembled from four complementary sources representing two biological domains - classical obesity susceptibility and organokine-mediated endocrine signalling.

Literature-derived SNPs. Candidate variants were identified from the GWAS Catalog (https://www.ebi.ac.uk/gwas/home). The complete catalog of published GWAS associations related to obesity and adiposity traits was downloaded and filtered in Python using the pandas

data-analysis library (https://pandas.pydata.org/). Variants annotated to obesity-related traits, including body mass index, waist circumference, and obesity, were retained for the obesity-susceptibility panel [19, 20, 22-24]. Variants associated with organokine-related traits, including adipokine, myokine, hepatokine, and individual organokine-encoding genes and circulating biomarkers such as leptin, adiponectin, and interleukin-6, were retained for the organokine-associated panel list [25-29].

Candidate gene regions. Genomic coordinates were extracted for 20 a priori selected obesity-susceptibility genes (*FTO*, *LEPR*, *PCSK1*, *LEP*, *SIM1*, *MC4R*, *PPARG*, *POMC*, *ESR1*, *CD36*, *ELOVL6*, *ADIPOQ*, *ENPP1*, *IRS2*, *CLOCK*, *MGLL*, *ADIPOR2*, *UCP3*, *PPARD,* and *EXOC4*) [19-23] and 20 organokine-encoding genes (*PPARGC1A*, *IL15*, *IGF1*, *BDNF*, *AGXT2*, *CTSB*, *SPARC*, *FETUB*, *ADIPOQ*, *LDHA*, *LEP*, *ERFE*, *FNDC5*, *AHSG*, *FST*, *MSTN*, *APLN*, *IL6*, *IL10*, and *OSM*) [24-28]. Gene coordinates were expanded by ±20 kilobase (kb) upstream and downstream using BCFtools (https://samtools.github.io/bcftools/bcftools.html) to capture variants located within potentially regulatory flanking regions.

Variants obtained from the literature-derived SNP panels and each set of gene-flanking-region variants was subsequently intersected with the genotyped variant positions on the Illumina Global Screening Array to retain only variants present in the study dataset.

Figure 1 provides an overview of the study workflow and analytical pipeline, including genotype-level quality control (n = 142), candidate variant prioritization (n = 2,652), five phenotype-specific genome-wide candidate variant association analyses, and cross-phenotype comparison of obesity- and organokine-associated variants.

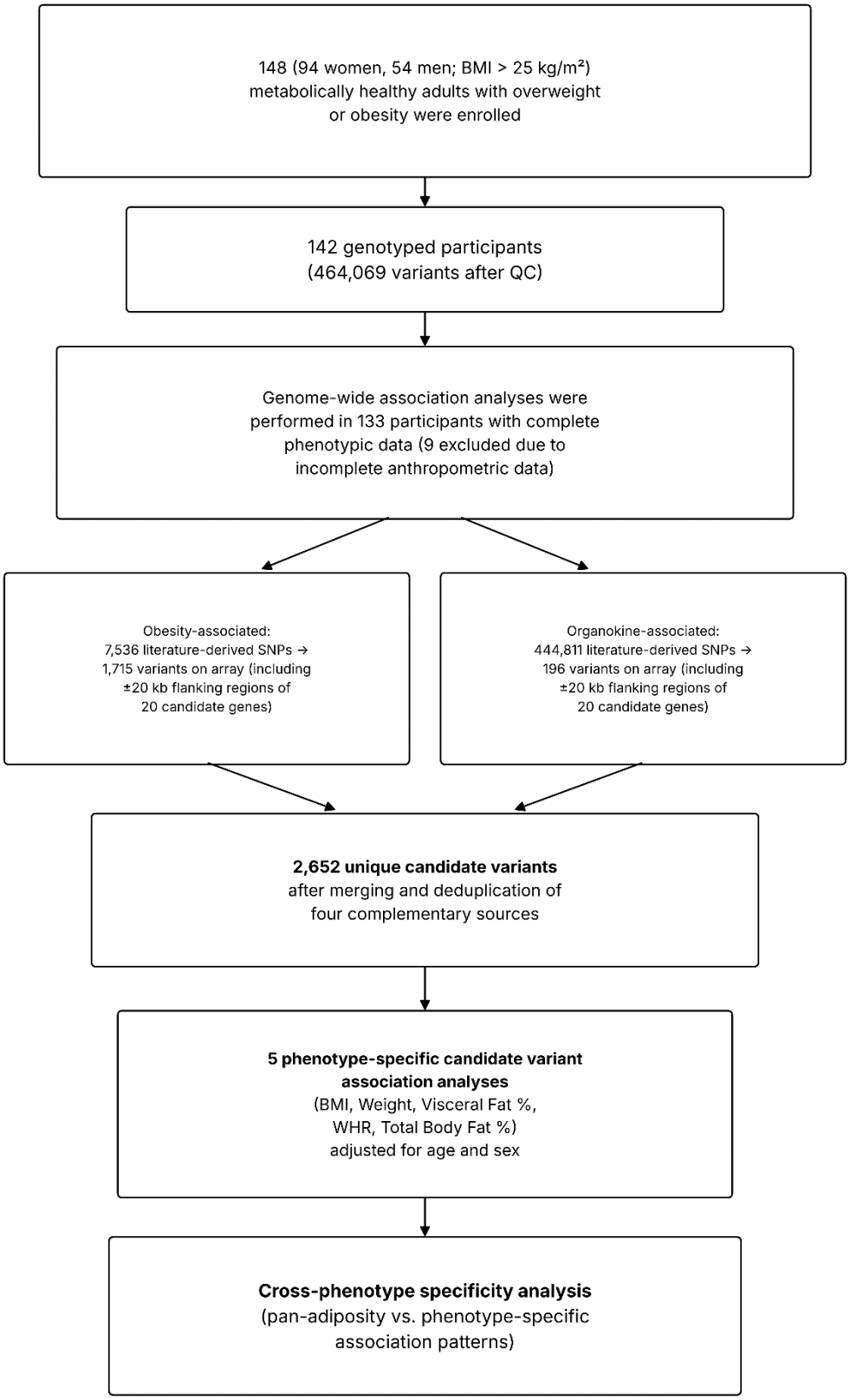

196

197 **Figure 1. S**tudy workflow and analytical pipeline.

Genotyping, Quality Control and Genome-Wide Association Study

Genomic DNA was isolated from peripheral blood leukocytes using the E.Z.N.A. Blood DNA Maxi Kit (Omega Bio-Tek, Norcross, GA, USA) following the manufacturer's protocol for up to 10 mL of whole blood. DNA concentration and purity were assessed using a NanoDrop ND-1000 spectrophotometer (Thermo Fisher Scientific, Massachusetts, USA).

Genotyping was performed using the Illumina Global Screening Array (GSA), generating genotype calls for 654,027 variants across 142 individuals prior to quality control (QC). QC was conducted in PLINK v1.9 following standard sequential steps. Variant-level QC included assessment of missingness (--missing), exclusion of variants with a call rate below 95% (--geno 0.05), minor allele frequency below 1% (--maf 0.01), and deviation from Hardy-Weinberg equilibrium ($p < 1\times10^{-6}$) (--hwe 1e-6). Sample-level QC included exclusion of individuals with more than 5% missing genotypes (--mind 0.05), evaluation of pairwise identity-by-descent to identify unexpected relatedness or duplicate samples (--genome), and removal of heterozygosity outliers (--het). Following QC, 142 individuals and 464,069 variants passed filtering and were retained for downstream analyses.

Statistical Software. All genotype quality control and association analyses were performed using PLINK v1.9. Data processing, statistical analysis, and visualization were conducted in R (R Core Team) using the packages *dplyr, tidyr, ggplot2, ggrepel, qqman*, and *gtsummary*.

Genome-Wide Association Study (GWAS). Genome-wide association analyses were performed for each of the five adiposity-related phenotypes using PLINK's linear regression (--linear) across all 464,069 variants that passed QC. An additive genetic model was applied, with the effect of each variant on the phenotype estimated while adjusting for age and sex as covariates. Ninety-five percent confidence intervals (CI) for effect estimates (β) were calculated using the --ci 0.95 option. Genomic inflation factors (λ) were derived from the

median chi-squared statistic to assess residual population stratification in each phenotype-specific analysis. All five analyses yielded λ values close to unity (λ=1.029-1.142), indicating minimal genomic inflation and no evidence of substantial residual population stratification.

Minor Allele Frequency Filtering. Minor allele frequency (MAF) was calculated for all candidate variants using PLINK's --freq function. To reduce the likelihood of unstable effect estimates arising from rare variants in a relatively modest sample, variants with MAF < 0.05 were excluded from the primary reporting of top associated candidate loci for each phenotype. However, all association results, including those for low-frequency variants, were retained for completeness and supplementary interpretation.

Multiple Testing Correction. Because the primary objective was to evaluate a predefined panel of biologically informed candidate variants, multiple-testing correction was applied only to the candidate variant panel (n = 2,652) extracted from the genome-wide association analyses rather than to the full genome-wide dataset. Bonferroni correction and the Benjamini-Hochberg false discovery rate (FDR) procedure were implemented in R using the p.adjust() function. Statistical significance within the candidate panel was defined as an FDR-adjusted q-value (Q) < 0.05. Variants with unadjusted p-values < 0.05 that did not remain significant after multiple-testing correction were considered nominally or suggestively associated.

Linkage Disequilibrium Assessment. For genomic regions in which multiple statistically significant or nominally associated variants clustered within the same locus, pairwise linkage disequilibrium (LD) was assessed using PLINK's --r2 function. This analysis was performed to determine whether the observed associations represented independent signals or reflected a shared underlying haplotype structure. Particular attention was given to the *IL6* locus on chromosome 7, where several associated variants were identified.

Extraction of Candidate Variant Association Statistics. Association statistics (β, standard error, 95% confidence interval, and p-value) for all 2,652 candidate variants were

extracted directly from the genome-wide association analyses performed for each phenotype. No separate candidate-panel-specific association analysis was conducted. This approach ensured that all candidate variant results were derived from a single, internally consistent statistical model for each phenotype, thereby avoiding potential discrepancies that could arise from re-estimating association statistics in a separately filtered dataset. Of the 2,652 retained candidate variants, 798 were identified exclusively through gene-region mapping, 1,539 originated solely from literature-derived SNPs lists, and 315 were supported by both approaches.

RESULTS

A total of 148 metabolically healthy adults with overweight or obesity (94 women and 54 men) were recruited for the study. Following genotyping quality-control procedures, 142 individuals remained eligible for genetic analyses, yielding a dataset of 464,069 quality-controlled variants. Complete phenotypic data were available for 133 participants (88 women and 45 men, BMI 32.7 ± 5.4 kg/m², aged 39.6 ± 8.5 years), who were included in subsequent phenotype-specific association analyses.

Integration of literature-derived obesity-associated and organokine-associated variants with variants located within predefined candidate gene regions resulted in a final panel of 2,652 unique candidate variants, which were subsequently evaluated across five adiposity-related phenotypes. The overall study workflow and analytical pipeline are presented in Figure 1.

Candidate variant panel construction

A non-redundant panel of 2,652 candidate variants was constructed from four complementary sources, including obesity-associated SNPs, organokine-associated SNPs, variants located within ±20 kb of obesity-susceptibility genes, and variants located within ±20 kb of organokine-encoding genes. Cross-referencing GWAS Catalog-derived variant lists (see

Methods, Section 2.3) with the Illumina Global Screening Array identified 1,715 of 7,536 obesity-associated SNPs and 196 of 444,811 organokine-associated SNPs, while gene-region mapping contributed an additional 1,140 variants across 40 candidate genes. The substantially larger unfiltered organokine-associated SNP pool reflects the broader range of trait terms used to query the GWAS Catalog for this biological domain (Methods, Section 2.3), rather than differences in data quality or extraction procedures.

Following deduplication across all sources, a final panel of 2,652 unique candidate variants was retained for downstream analyses (Table 1). Of the 399 variants identified across multiple sources, 315 (11.9%) were supported by both a candidate gene region and an independent literature-derived SNP list. Overall, 798 (30.1%) variants were identified exclusively through gene-region mapping, whereas 1,539 (58.0%) originated solely from literature-derived SNP lists. Variants were further annotated according to both their source category (literature-based SNP list, candidate gene region, or both) and biological pathway classification (obesity-related, organokine-related, or both). Several variants were assigned to overlapping biological categories, particularly within loci encoding adipokines such as *ADIPOQ* and *LEP*.

The final candidate variant panel was subsequently evaluated for associations with five adiposity-related phenotypes using summary statistics extracted from genome-wide association analyses performed in 133 participants with complete phenotypic data.

Table 1. Sources of candidate variants and final candidate panel composition

Source	**Initial source size /** Total variants identified	**Variants present on genotyping array** (variants retained in study dataset)
Obesity-associated SNPs (literature-derived, NCBI)	7,536	1,715

Organokine-associated SNPs (literature-derived, NCBI)	444,811	196
Variants within ±20 kb of 20 obesity candidate genes and 20 organokine candidate genes	40 genes	1,140
Total candidate variants before deduplication	NA	**3,051**
Overlapping variants identified from multiple sources	NA	**399**
Total unique candidate variants after deduplication	NA	**2,652**

294

295 **Phenotype-Specific Candidate Variant Associations**

296 Table 1 summarizes the results of the candidate variant association analysis across all five
297 adiposity-related phenotypes. The number of nominally associated variants ($p < 0.05$) ranged
298 from 116 to 152 across phenotypes, representing to 4.3-5.7% of the 2,652 candidate variants
299 evaluated. Body weight was the only phenotype for which candidate variants remained
300 statistically significant after false discovery rate (FDR) correction, with two variants meeting
301 the significance threshold. No variants associated with BMI, visceral fat percentage, waist-to-
302 hip ratio, or total body fat percentage survived multiple-testing correction. The largest numbers
303 of nominally associated variants were observed for total body fat percentage (n = 152) and
304 BMI (n = 143), whereas waist-to-hip ratio showed the fewest nominal associations (n = 116).
305 Across phenotypes, the most frequently represented loci among the top 15 nominally associated
306 variants (ranked by lowest p-value) for each phenotype included *IL6*, *FTO*, *LDHA*, *SPARC*,
307 and *POMC* (Tables 3-7). Genomic inflation factors ranged from 1.029 to 1.142, indicating
308 minimal residual population stratification and acceptable control of test statistic inflation across
309 across all phenotype-specific analyses. Candidate-panel-specific Bonferroni and FDR

correction thresholds are presented in Table 2. The complete set of analyses was performed using the same panel of 2,652 unique candidate variants.

Table 2. Summary of phenotype-specific candidate variant association analyses across five adiposity-related phenotypes

Phenotype	Nominal associations **(%) p<0.05**	**Low-frequency** variants **(MAF < 0.05)**	**λ (GC)**	Variants significant after FDR correction	**Top locus/loci**
BMI	143 (5.3%)	27	1.142	0	*IL6*
Weight	130 (4.8%)	28	1.097	2	*IL6*
Visceral fat, %	135 (5.0%)	22	1.127	0	*LDHA*, *FTO*
Waist-to-hip ratio	116 (4.3%)	11	1.038	0	*FTO*, *LDHA*
Total body fat, %	152 (5.7%)	22	1.029	0	*SPARC*, *POMC*

Abbreviations: *BMI, body mass index; MAF, minor allele frequency; FDR, false discovery rate; λGC, genomic inflation factor.* **Note:** Top loci represent genes containing the highest-ranking variants based on nominal association p-values.

Body Mass Index

Genotype–phenotype association testing for BMI was performed in 133 participants with complete phenotypic data. Each of the 2,652 candidate variants was evaluated individually under an additive genetic model adjusted for age and sex. A total of 143 variants (5.3%) showed nominal evidence of association with BMI ($p < 0.05$). However, none remained statistically significant after Bonferroni or FDR correction (all $Q \geq 0.05$). For descriptive reporting of the top-ranked associations, variants with MAF < 0.05 (n = 27) were excluded

to minimize potential instability of effect estimates. The strongest association was observed for rs2069845 in *IL6* (β = 2.31, 95% CI: 1.08-3.54, p = 3.4×10^{-4}), although the association did not remain significant after multiple-testing correction (Q = 0.233). Notably, six of the top 15 variants mapped to the *IL6* locus on chromosome 7, indicating a regional concentration of association signals (Table 3). Linkage disequilibrium (LD) analysis indicated that these variants formed a correlated association cluster, suggesting a shared haplotype signal rather than multiple independent effects. A secondary cluster of variants on chromosome 15 comprised two pairs in complete linkage disequilibrium (rs588765-rs680244 and rs615470-rs660652; $r^2 = 1.0$ within each pair), with strong linkage disequilibrium between the two pairs ($r^2 = 0.79$), consistent with a single shared haplotype block. All four variants exhibited similar negative effect estimates, supporting the interpretation of a common underlying haplotype signal, however, none remained significant after FDR correction.

Table 3. Top candidate-variant associations with body mass index ranked by nominal p-value among 133 metabolically healthy adults with overweight or obesity (MAF ≥ 0.05)

SNP	Chr	Position (bp)	Variant annotation	MAF	β (95% CI)	P value	FDR Q
rs2069845*	7	22,730,530	Intronic (*IL6)*	0.447	2.31 (1.08 to 3.54)	3.44×10^{-4}	0.233
rs588765	15	78,573,083	Intronic (*CHRNA5*)	0.423	-2.31 (-3.57 to -1.04)	4.88×10^{-4}	0.233
rs680244	15	78,578,946	Intronic (*CHRNA5*)	0.423	-2.31 (-3.57 to -1.04)	4.88×10^{-4}	0.233
rs7578597	2	43,505,684	Missense (*THADA*)	0.056	4.72 (2.11 to 7.33)	5.51×10^{-4}	0.233
rs1800795	7	22,727,026	Upstream (*IL6)*	0.475	2.19 (0.94 to 3.44)	8.13×10^{-4}	0.242
rs2069832*	7	22,727,814	Upstream (*IL6)*	0.475	2.02 (0.78 to 3.26)	1.76×10^{-3}	0.335
rs10499563**	7	22,720,869	Promoter (*IL6*)	0.176	2.77 (1.07 to 4.46)	1.79×10^{-3}	0.335

rs1800797	7	22,726,602	Upstream (*IL6)*	0.486	1.99 (0.77 to 3.22)	1.81×10^{-3}	0.335
rs231775	2	203,867,991	Missense (*CTLA4*)	0.419	-2.19 (-3.58 to -0.79)	2.62×10^{-3}	0.421
rs6969927**	7	22,713,254	Intronic (*IL6*)	0.176	2.62 (0.91 to 4.32)	3.13×10^{-3}	0.441
rs11715363	3	127,797,141	Intronic (*MGLL*)	0.144	2.71 (0.91 to 4.50)	3.74×10^{-3}	0.450
rs2239179	12	47,863,983	Intronic (*VDR*)	0.379	-1.99 (-3.32 to -0.67)	3.90×10^{-3}	0.450
rs727428	17	7,634,474	Non-coding (*SHBG*)	0.380	-1.80 (-3.00 to -0.59)	4.06×10^{-3}	0.450
rs615470	15	78,593,646	Intronic (*CHRNA3*), 3'UTR (*CHRNA5*)	0.373	-1.97 (-3.29 to -0.65)	4.19×10^{-3}	0.450
rs660652	15	78,595,490	Intronic (*CHRNA3*), downstream (*CHRNA5*)	0.373	-1.97 (-3.29 to -0.65)	4.19×10^{-3}	0.450

Abbreviations: *MAF, minor allele frequency; CI, confidence interval; FDR, false discovery rate; UTR, untranslated region. Unmarked SNPs were present in either the obesity-susceptibility or the organokine-pathway candidate SNP panel. *Variants present in both candidate SNP panels. **Variant not present in either candidate SNP panel but located within the ±20 kb flanking region of a candidate gene.*

Body Weight

Among 130 nominally associated variants (4.8%), two variants in *IL6* remained significant after FDR correction: rs2069845 (β = 8.38 kg per allele, 95% CI: 4.64-12.13, p = 2.38×10^{-5}, FDR Q=0.046) and rs1800795 (β = 8.31 kg, 95% CI: 4.52-12.10, p = 3.41×10^{-5}, FDR Q=0.046).

These variants were in strong linkage disequilibrium (r^2 = 0.87), suggesting that they represent a single underlying *IL6* association signal rather than two independent effects. Notably, this was the only locus showing statistically significant associations after FDR correction across all five phenotypes examined. Four additional *IL6* variants (rs1800797,

rs2069832, rs10499563, and rs68072554) were also among the top 15 associated candidate variants and demonstrated consistently positive effect estimates, further supporting a localized association signal within the *IL6* locus (Table 4). In addition, the chromosome 15 cluster comprising variants within the *CHRNA3/CHRNA5* region (r^2 = 0.79-1.0) reflected a shared haplotype structure rather than multiple independent association signals, consistent with the pattern observed for BMI.

Table 4. Top candidate variant associations with body weight (n = 133; MAF ≥ 0.05)

SNP	Chr	Position (bp)	Variant annotation	MAF	β (95% CI)	P value	FDR Q
rs2069845*	7	22,730,530	Intronic (*IL6)*	0.447	8.38 (4.64 to 12.13)	2.38×10^{-5}	**0.046**
rs1800795	7	22,727,026	Upstream (*IL6)*	0.475	8.31 (4.52 to 12.10)	3.41×10^{-5}	**0.046**
rs1800797	7	22,726,602	Upstream (*IL6)*	0.486	7.85 (4.14 to 11.57)	6.04×10^{-5}	0.054
rs2069832*	7	22,727,814	Upstream (*IL6)*	0.475	7.66 (3.89 to 11.43)	1.12×10^{-4}	0.075
rs7578597	2	43,505,684	Missense (*THADA*)	0.056	14.93 (6.84 to 23.02)	4.24×10^{-4}	0.227
rs7830933	8	23,745,811	Non-coding transcript (*NKX2-6, STC1*)	0.239	8.08 (3.56 to 12.61)	6.38×10^{-4}	0.227
rs588765	15	78,573,083	Intronic (*CHRNA5*)	0.423	-6.92(-10.86 to -2.99)	7.63×10^{-4}	0.227
rs680244	15	78,578,946	Intronic (*CHRNA5*)	0.423	-6.92 (-10.86 to -2.99)	7.63×10^{-4}	0.227
rs10499563	7	22,720,869	Regulatory / Promoter (*IL6*)	0.176	9.05 (3.81 to 14.30)	9.56×10^{-4}	0.256

rs615470	15	78,593,646	Intronic (*CHRNA3*), 3'UTR (*CHRNA5*)	0.373	-6.50 (-10.59 to -2.41)	2.28×10^{-3}	0.471
rs660652	15	78,595,490	Intronic (*CHRNA3*), downstream (*CHRNA5*)	0.373	-6.50 (-10.59 to -2.41)	2.28×10^{-3}	0.471
rs6969927	7	22,713,254	Intronic (*IL6*)	0.176	8.11 (2.82 to 13.39)	3.20×10^{-3}	0.568
rs6804842	3	25,064,946	Intronic (*RARB*)	0.359	-5.82 (-9.66 to -1.97)	3.62×10^{-3}	0.568
rs68072554	7	22,748,682	Intronic (*IL6*)	0.193	7.66 (2.52 to 12.79)	4.11×10^{-3}	0.568
rs17145738	7	73,568,544	3'UTR (*TBL2*)	0.127	-8.74 (-14.69 to -2.79)	4.67×10^{-3}	0.568

Abbreviations: *MAF, minor allele frequency; CI, confidence interval; FDR, false discovery rate. UTR, untranslated region, Unmarked SNPs were present in either the obesity-susceptibility or the organokine-pathway candidate SNP list. *Variant listed in both the obesity-susceptibility and organokine-pathway candidate SNP lists*.

Visceral Fat Percentage

Of the 135 nominally associated variants (5.0%), none remained significant after correction for multiple testing. After filtering out low-frequency variants (MAF < 0.05), the strongest associations were observed for rs72868518 in *LDHA* (β=-1.97, 95% CI: -3.04 to -0.90, $p = 4.5\times10^{-4}$, MAF = 0.063), an organokine-related candidate gene, and rs16952686 in *FTO* locus (β = -1.99, 95% CI: -3.10 to -0.88, $p = 6.1\times10^{-4}$, MAF = 0.053), a well-established obesity-susceptibility gene (Table 5, Figure 4).

In addition, a cluster of correlated variants within *CHRNA3/CHRNA5* region on chromosome 15 (rs588765, rs680244, rs615470, and rs660652) showed consistently negative effect estimates for visceral fat percentage, although none survived FDR correction. As

observed for BMI and body weight, these variants (in chromosome 15 cluster) were in strong linkage disequilibrium (r^2 = 0.79-1.0), suggesting a shared haplotype structure rather than independent suggesting signals. The obesity-related gene *PCSK1* was also represented among the top associations through rs156002 ($\beta = -0.79$, 95% CI: −1.34 to −0.25, $p = 4.95\times10^{-3}$).

Table 5. Top candidate variant associations with visceral fat percentage (n = 133; MAF ≥ 0.05)

SNP	Chr	Position (bp)	Variant annotation	MAF	β (95% CI)	P value	FDR Q
rs72868518	11	18,391,640	Intronic (*LDHA)*	0.063	-1.97 (-3.04 to -0.90)	4.52×10^{-4}	0.817
rs16952686	16	53,955,761	Intronic (*FTO)*	0.053	-1.99 (-3.10 to -0.88)	6.09×10^{-4}	0.817
rs11826287	11	68,379,193	Intronic (*LRP5)*	0.144	1.15 (0.45 to 1.85)	1.61×10^{-3}	0.820
rs588765	15	78,573,083	Intronic (*CHRNA5*)	0.423	-0.77 (-1.25 to -0.30)	1.84×10^{-3}	0.820
rs680244	15	78,578,946	Intronic (*CHRNA5*)	0.423	-0.77 (-1.25 to -0.30)	1.84×10^{-3}	0.820
rs7830933	8	23,745,811	Non-coding transcript (*NKX2-6, STC1*)	0.239	0.88 (0.33 to 1.43)	2.20×10^{-3}	0.820
rs4845625	1	154,449,591	Intronic (*IL6R*)	0.479	-0.78 (-1.29 to -0.28)	2.94×10^{-3}	0.820
rs564343	11	66,127,695	Intronic (*PACS1*)	0.497	0.69 (0.24 to 1.15)	3.54×10^{-3}	0.820
rs615470	15	78,593,646	Intronic (*CHRNA3*), 3'UTR (*CHRNA5*)	0.373	-0.74 (-1.23 to -0.24)	4.13×10^{-3}	0.820
rs660652	15	78,595,490	Intronic (*CHRNA3*),	0.373	-0.74 (-1.23 to -0.24)	4.13×10^{-3}	0.820

			downstream (*CHRNA5*)				
rs6982502	8	125,467,120	Intronic (*TRIB1AL*)	0.331	0.78 (0.25 to 1.32)	4.53×10^{-3}	0.820
rs35262691	14	94,518,729	Upstream (*SERPINA12*)	0.426	-0.68 (-1.15 to -0.22)	4.90×10^{-3}	0.820
rs156002	5	96,446,870	Intronic (*PCSK1*)	0.444	-0.79 (-1.34 to -0.25)	4.95×10^{-3}	0.820
rs7846385	8	77,247,943	Intergenic (*HIGD1AP18, PKIA*)	0.268	-0.76 (-1.29 to -0.24)	5.01×10^{-3}	0.820
rs1409874	10	6,608,464	Non-coding transcript (*LINP1*)	0.176	0.84 (0.25 to 1.42)	5.71×10^{-3}	0.820

Abbreviations: *MAF, minor allele frequency; CI, confidence interval; FDR, false discovery rate; UTR, untranslated region.*

Waist-to-Hip Ratio

Among 116 nominally associated variants (4.3%), none remained significant after correction for multiple testing. The strongest associations were observed for rs16952686 in *FTO* (β = -0.065, 95% CI: -0.104 to -0.025, p = 1.8×10^{-3}) and rs156002 in *PCSK1* (β = -0.030, 95% CI: -0.049 to -0.011, p = 2.6×10^{-3}), both obesity-susceptibility candidate genes. The *LDHA* variant rs72868518 was also among the top 15 associated variants (β = -0.058, p = 3.7×10^{-3}), consistent with its appearance among the strongest signals for visceral fat percentage (Table 6, Figure 4).

A pair of correlated variants within the *CHRNA5* locus on chromosome 15 (rs588765 and rs680244) also showed consistent negative effect estimates for waist-to-hip ratio. As observed for BMI and visceral fat percentage these variants were in strong linkage disequilibrium (r^2 = 0.79-1.0), suggesting a shared haplotype structure rather than independent association signals.

406 **Table 6**. Top candidate variant associations with waist-to-hip ratio (n = 133; MAF ≥ 0.05)

SNP	Chr	Position (bp)	Variant annotation	MAF	β (95% CI)	P value	FDR Q
rs16952686	16	53,955,761	Intronic (*FTO*)	0.053	-0.065 (-0.104 to -0.025)	1.76×10^{-3}	0.944
rs156002	5	96,446,870	Intronic (*PCSK1*)	0.444	-0.030 (-0.049 to -0.011)	2.62×10^{-3}	0.944
rs7474896	10	37,693,169	Non-coding transcript (*ZNF248*, *MTND1P18*)	0.121	-0.041 (-0.068 to -0.015)	2.75×10^{-3}	0.944
rs4684677	3	10,286,769	Missense (*GHRL*) / Intronic (*GHRLOS*)	0.099	0.045 (0.016 to 0.075)	3.08×10^{-3}	0.944
rs72868518	11	18,391,640	Intronic (*LDHA*)	0.063	-0.058 (-0.097 to -0.02)	3.69×10^{-3}	0.944
rs11826287	11	68,379,193	Intronic (*LRP5)*	0.144	0.038 (0.013 to 0.062)	3.77×10^{-3}	0.944
rs7431368	3	128,472,098	Non-coding transcript (*DNAJB8*)	0.201	0.031 (0.010 to 0.052)	4.15×10^{-3}	0.944
rs1536475	9	134,429,310	Intronic (*RXRA*)	0.166	-0.034 (-0.057 to -0.011)	4.21×10^{-3}	0.944
rs35262691	14	94,518,729	Upstream (*SERPINA12*)	0.426	-0.025 (-0.041 to -0.008)	4.23×10^{-3}	0.944
rs7830933	8	23,745,811	Non-coding transcript (*NKX2-6, STC1*)	0.239	0.029 (0.009 to 0.048)	4.86×10^{-3}	0.944
rs588765	15	78,573,083	Intronic (*CHRNA5*)	0.423	-0.024 (-0.041 to -0.007)	6.81×10^{-3}	0.944
rs680244	15	78,578,946	Intronic (*CHRNA5*)	0.423	-0.024 (-0.041 to -0.007)	6.81×10^{-3}	0.944

rs4845625	1	154,449,591	Intronic (*IL6R*)	0.479	-0.025 (-0.043 to -0.007)	8.29×10^{-3}	0.944
rs564343	11	66,127,695	Intronic (*PACS1*)	0.497	0.022 (0.006 to 0.038)	9.28×10^{-3}	0.944
rs2550948	5	1,450,329	Non-coding transcript (*LPCAT1*)	0.475	0.021 (0.005 to 0.037)	1.05×10^{-2}	0.944

Abbreviations: *MAF, minor allele frequency; CI, confidence interval; FDR, false discovery rate.*

Total Body Fat Percentage

Of the 152 nominally associated variants (5.7%), none remained significant after correction for multiple testing. Among candidate-gene variants, the strongest associations after MAF filtering were observed for rs11167552 in *SPARC* (β = -1.83, 95% CI: -2.88 to -0.79, p = 8.0×10^{-4}), an organokine candidate gene, and rs72868518 in *LDHA* (β = −3.92, 95% CI: −6.26 to −1.59, p = 1.28×10^{-3}) another organokine-pathway candidate gene. Variants within *POMC* (rs72810013) and the neighboring *EFR3B* region (rs13428823) were among the strongest obesity-related associations, while two independent variants within the *SPARC* locus (rs1059829 and rs1059829), and rs2077647 in *ESR1* represented additional leading signals. Together, these findings highlight the contribution of both obesity-susceptibility and organokine-related loci to variation in total body fat percentage (Table 7). Notably, rs72868518 in *LDHA* appeared among the leading associations for three adiposity-related phenotypes - total body fat percentage, visceral fat percentage, and waist-to-hip ratio.

Table 7. Top candidate variant associations with total body fat percentage (n = 133; MAF ≥ 0.05)

SNP	Chr	Position (bp)	Variant annotation	MAF	β (95% CI)	P value	FDR Q
rs572169	3	172,447,937	Synonymous (*GHSR*)	0.278	-2.06 (-3.11 to -1.01)	1.88×10^{-4}	0.505
rs509035	3	172,445,659	Intronic (*GHSR*)	0.285	-1.99 (-3.01 to -0.97)	2.06×10^{-4}	0.554
rs1409874	10	6,608,464	Non-coding transcript (*LINP1*)	0.176	2.24 (1.00 to 3.48)	5.54×10^{-4}	0.450
rs11167552	5	151,647,586	Intronic *(SPARC)*	0.412	-1.83 (-2.88 to -0.79)	7.99×10^{-4}	0.450
rs231775	2	203,867,991	Missense (*CTLA4*)	0.419	-1.95 (-3.06 to -0.83)	8.75×10^{-4}	0.450
rs72868518	11	18,391,640	Intronic *(LDHA)*	0.063	-3.92 (-6.26 to -1.59)	1.28×10^{-3}	0.450
rs11826287	11	68,379,193	Intronic (*LRP5)*	0.144	2.53 (1.02 to 4.04)	1.31×10^{-3}	0.450
rs1866146	2	25,157,704	3'UTR *(EFR3B)*	0.409	-1.71 (-2.73 to -0.68)	1.40×10^{-3}	0.450
rs72810013	2	25,180,938	Intronic (*POMC)*	0.254	-2.02 (-3.24 to -0.80)	1.51×10^{-3}	0.450
rs13428823	2	25,150,429	Intronic *(EFR3B)*	0.440	-1.63 (-2.62 to -0.63)	1.71×10^{-3}	0.460
rs6982502	8	125,467,120	Intronic (*TRIB1AL*)	0.331	1.85 (0.70 to 2.99)	1.95×10^{-3}	0.475
rs1059829	5	151,662,468	3'UTR *(SPARC)*	0.475	1.65 (0.61 to 2.68)	2.30×10^{-3}	0.501
rs2077647	6	151,807,942	Synonymous *(ESR1)*	0.430	-1.70 (-2.77 to -0.62)	2.43×10^{-3}	0.501
rs12785878	11	71,456,403	Intronic (*NADSYN1*)	0.359	1.81 (0.65 to 2.97)	2.79×10^{-3}	0.534

rs3749147	2	27,629,051	Non-coding transcript (*GPN1*) / Upstream (*CCDC121*)	0.218	-1.90 (-3.15 to -0.66)	3.34×10^{-3}	0.598

Abbreviations: *MAF, minor allele frequency; CI, confidence interval; FDR, false discovery rate; UTR, untranslated region. β denotes the additive effect estimate per copy of the minor allele, adjusted for age and sex.*

Convergent Evidence Across Candidate Genes and Phenotypes

Several candidate genes showed consistent, phenotype-selective patterns of association across the five analyses (Figure 3). *IL6* variants were repeatedly among the top 15 associated loci for BMI and body weight, the two overall body mass phenotypes, including the sole FDR-significant finding in this study, but did not appear among the top 15 signals for visceral fat percentage, WHR, or total body fat percentage. Conversely, *LDHA* (rs72868518) was among the top 15 associated loci for (visceral fat percentage, WHR, and total body fat percentage, but not for BMI or body weight (Figure 4). Likewise, *FTO* (rs16952686) appeared among the leading associations for visceral fat percentage and WHR. *POMC* and *SPARC* variants were associated specifically with total body fat percentage and did not appear among the top signals for any other phenotype. This gene-level convergence, observed independently across the five phenotype-specific analyses, suggests partially distinct patterns of association for overall body mass versus fat distribution and body composition phenotypes.

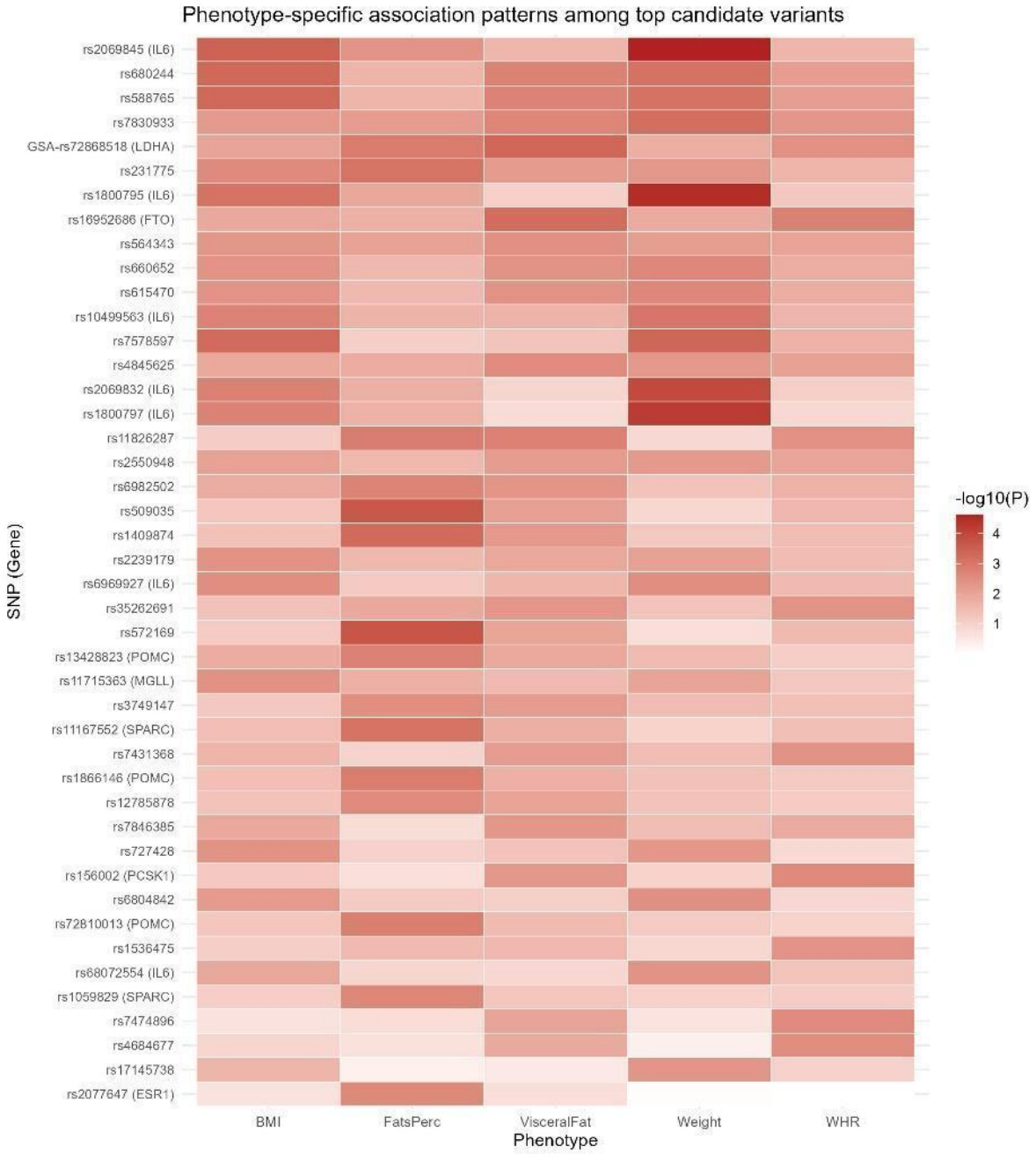

448

449 **Figure 3.** Heatmap of phenotype-specific association strength (-log10 p-value) for selected top
450 candidate variants across five adiposity-related phenotypes (BMI, total body fat percentage
451 (FatsPerc), visceral fat percentage (VisceralFat), weight, and waist-to-hip ratio (WHR)).
452 Darker shading indicates stronger nominal association.

453

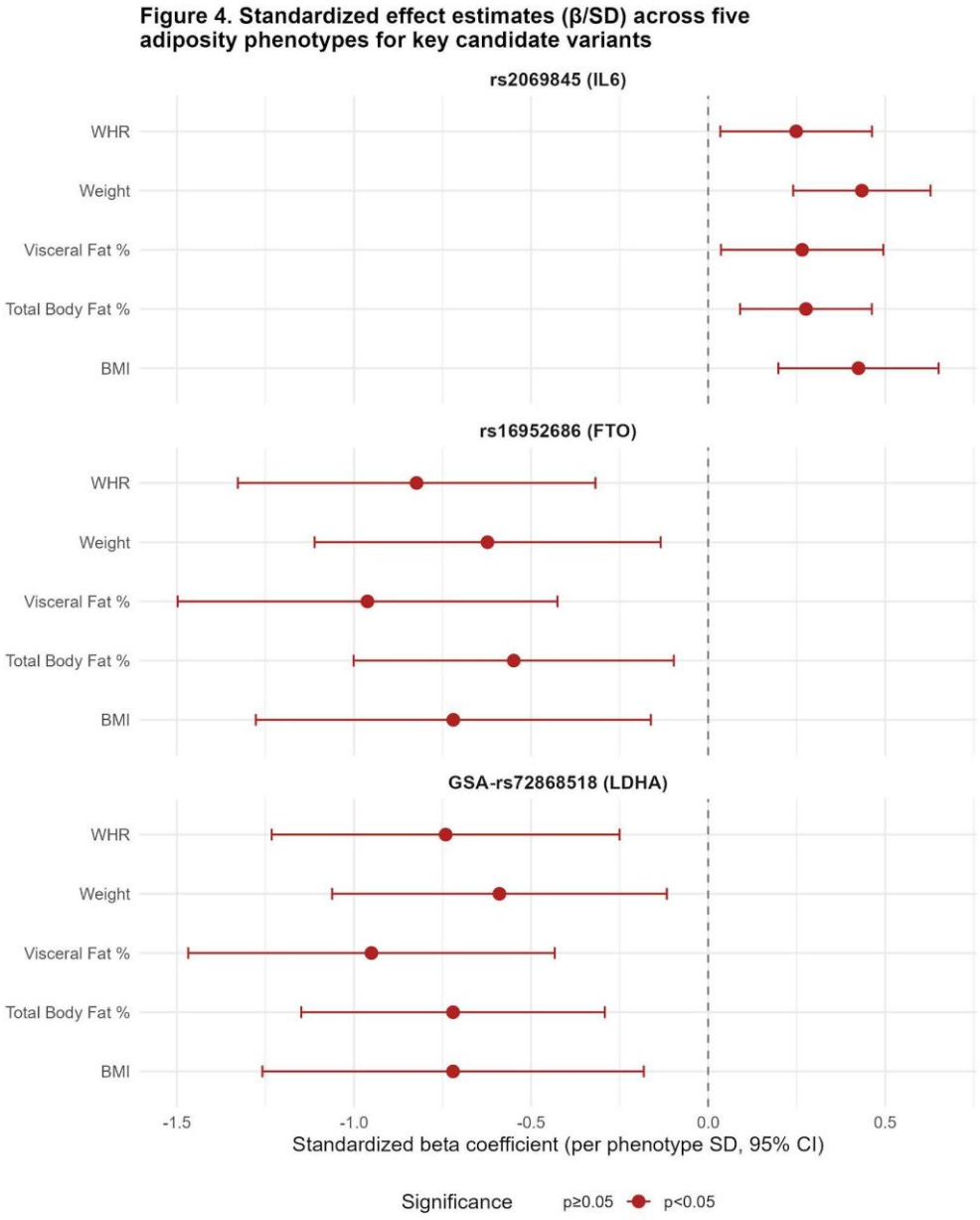

454

455 **Figure 4.** Standardized effect estimates (β per phenotype standard deviation, with 95%
456 confidence intervals) across five adiposity phenotypes for representative *IL6* (rs2069845), *FTO*
457 (rs16952686), and *LDHA* (rs72868518) variants. *IL6* demonstrated consistently positive effect
458 estimates across all five phenotypes, whereas *FTO* and *LDHA* demonstrated consistently
459 negative effect estimates, with the largest standardized effects observed for visceral fat
460 percentage and WHR.

461

462 Phenotype-specificity patterns for obesity-associated and organokine-pathway variants
463 (MAF ≥ 0.05) are summarized in Table 8. A higher proportion of organokine-pathway variants

exhibited broad (3-4 phenotypes) or pan-adiposity (all 5 phenotypes) association patterns compared with obesity-susceptibility variants, although this difference did not reach statistical significance (Fisher's exact test, p = 0.390).

Table 8. Comparison of phenotype-specificity patterns between obesity-associated and organokine pathway variants (MAF ≥ 0.05)

Specificity pattern	Obesity-associated variants (N=446)	Organokine-pathway variants (N=251)
Not associated with any phenotype	409 (91.7%)	215 (85.7%)
Phenotype-specific (1-2 phenotypes)	30 (6.7%)	25 (10.0%)
Broad (3-4 phenotypes)	6 (1.3%)	7 (2.8%)
Pan-adiposity (all 5 phenotypes)	1 (0.2%)	4 (1.6%)

Phenotype specificity was defined according to the number of adiposity phenotypes showing nominal association ($p < 0.05$) for a given variant.

DISCUSSION

This study combined detailed adiposity phenotyping with genome-wide association analyses and targeted evaluation of literature-derived obesity-susceptibility and organokine-pathway genetic variants in a cohort of metabolically healthy Lithuanian adults with overweight or obesity. By examining five complementary adiposity-related phenotypes, including measures of overall body mass, fat distribution, and body composition, we aimed to characterize phenotype-specific and pleiotropic association patterns and to gain insight into the genetic architecture underlying different dimensions of adiposity.

The results revealed phenotype-specific patterns of genetic association, suggesting that the genetic architecture of obesity may vary according to the adiposity trait being measured. Distinct candidate genes preferentially associated with different adiposity phenotypic domains,

with *IL6* variants primarily linked to overall body mass measures (BMI and body weight), *FTO* and *LDHA* variants preferentially associated with fat distribution and body-composition phenotypes, and *POMC* and *SPARC* variants associated specifically with total body fat percentage. These findings supports our first hypothesis and are consistent with the growing recognition that obesity represents a heterogeneous biological condition comprising multiple partially overlapping molecular and physiological pathways rather than a single unified trait [29,30]**.** The observed phenotype-specific associations are biologically plausible and suggest that inflammatory signaling (*IL6*), central appetite regulation (*POMC*), energy metabolism (*LDHA* and *FTO*), and extracellular matrix remodeling (*SPARC*) may contribute differentially to distinct dimensions of adiposity [16, 30-33].

An important feature of the present study is its focus on metabolically healthy adults with overweight or obesity. Unlike many genetic studies conducted in populations enriched for diabetes, metabolic syndrome, or other obesity-related complications, this design aimed to investigate adiposity-related genetic variation in the relative absence of overt metabolic dysfunction. Such an approach may help disentangle genetic factors associated with adiposity itself from those related primarily to downstream metabolic complications. Consequently, the observed associations may more directly reflect biological mechanisms underlying body fat accumulation and distribution rather than secondary disease-related processes.

The most robust finding of this study was the identification of the *IL6* locus as the only association that remained significant after correction for multiple testing. Multiple correlated *IL6* variants were among the strongest signals for both BMI and body weight, with rs2069845 and rs1800795 demonstrating FDR-significant associations with body weight. This observation is biologically plausible because interleukin-6 is a multifunctional cytokine secreted by adipose tissue, skeletal muscle, and immune cells and plays a central role in the regulation of inflammatory and metabolic processes. Elevated circulating IL-6 concentrations have

consistently been associated with obesity, adipose tissue expansion, insulin resistance, and chronic low-grade inflammation [34, 35]. The consistent positive direction of effect observed across all five adiposity phenotypes further supports the involvement of IL-6-related pathways in overall adiposity. Notably, the strongest associations were observed for BMI and body weight rather than indices of fat distribution, suggesting that inflammatory signaling may be more closely linked to total body mass accumulation than to regional fat deposition patterns.

The phenotype-specific association patterns observed in this study reinforce the view that obesity should not be considered a single homogeneous trait. Although BMI, body weight, visceral fat percentage, waist-to-hip ratio, and total body fat percentage are correlated measures, they capture distinct aspects of adiposity biology and may therefore reflect partially different biological pathways. The observation that *IL6* was primarily associated with overall body mass, whereas *FTO* and *LDHA* were more strongly related to fat distribution and body composition, highlights the value of multidimensional adiposity phenotyping. Had the analyses been restricted to BMI alone, several potentially informative phenotype-specific associations would not have been identified.

In contrast to *IL6*, variants within *FTO* and *LDHA* preferentially associated with phenotypes reflecting fat distribution and body composition. The representative *FTO* variant rs16952686 was among the strongest associations for visceral fat percentage and waist-to-hip ratio and demonstrated larger standardized effect estimates for these phenotypes than for overall body mass measures. This observation is consistent with previous reports suggesting that *FTO* variation influences not only general adiposity but also patterns of regional fat accumulation and visceral adiposity [31]**.** Because visceral fat is more strongly associated with cardiometabolic risk than total adiposity, these findings further emphasize the importance of evaluating obesity-related traits beyond BMI alone.

The repeated appearance of rs72868518 within *LDHA* across visceral fat percentage, waist-to-hip ratio, and total body fat percentage represents one of the most intriguing findings of the present study. *LDHA* encodes lactate dehydrogenase A, a key glycolytic enzyme involved in lactate production and cellular energy metabolism [14, 36]**.** Although *LDHA* has received relatively limited attention in obesity genetics, emerging evidence suggests that lactate metabolism contributes to adipose tissue function, metabolic flexibility, and whole-body energy homeostasis. The consistent association of rs72868518 across multiple measures of body composition raises the possibility that variation within glycolytic pathways may influence patterns of fat deposition and adipose tissue distribution. Given the limited genetic literature linking *LDHA* to adiposity-related phenotypes, this finding should be regarded as hypothesis-generating and warrants replication in independent cohorts together with functional investigation.

An additional noteworthy finding was the phenotype specificity observed for *POMC* and *SPARC*. Three independent *POMC* variants and two *SPARC* variants were among the strongest associations for total body fat percentage yet did not appear among the leading signals for BMI, body weight, visceral fat percentage, or waist-to-hip ratio. This pattern is biologically plausible given the distinct functions of these genes. *POMC* encodes a precursor of melanocortin peptides that play a central role in hypothalamic appetite regulation and energy balance, whereas *SPARC* (secreted protein acidic and rich in cysteine, also known as osteonectin) contributes to extracellular matrix remodeling, adipose tissue architecture, and tissue fibrosis [29, 32, 37-39]**.** The identification of these loci specifically in relation to total body fat percentage suggests that some genetic determinants preferentially influence adipose tissue quantity and composition rather than total body mass. These findings further reinforce the concept that anthropometric and body-composition traits, although closely related, are not genetically interchangeable phenotypes.

The comparison between obesity-susceptibility and organokine-pathway variants provided additional insight into the biological organization of adiposity-related genetic variation. Organokine-pathway variants demonstrated a numerically greater tendency toward broad or pan-adiposity associations than classical obesity-susceptibility variants, although the difference did not reach statistical significance. Organokines serve as key mediators of inter-organ communication and regulate numerous processes relevant to obesity, including adipose tissue expansion, energy expenditure, inflammation, insulin sensitivity, and metabolic adaptation [14-16]**.** Through endocrine, paracrine, and autocrine signaling mechanisms, organokines coordinate physiological responses across adipose tissue, skeletal muscle, liver, bone, and other metabolically active organs [14-16]. Consequently, genetic variation within organokine-related pathways may be expected to influence multiple dimensions of adiposity simultaneously. The tendency toward broader phenotypic involvement observed among organokine-pathway variants in the present study is therefore biologically consistent with this emerging framework, even though statistical significance was not achieved. Because the number of variants demonstrating any phenotypic association was relatively small, statistical power to detect differences between groups was limited, and these findings should be interpreted as exploratory rather than confirmatory.

The absence of significant associations for many previously reported obesity-related variants should also be interpreted cautiously. Genetic effects on adiposity-related traits are often modest and may vary according to population characteristics, environmental exposures, phenotype definition, linkage disequilibrium structure, and study design. Furthermore, the present cohort consisted exclusively of metabolically healthy adults with overweight or obesity, a population that may differ biologically from cohorts included in large-scale obesity genome-wide association studies. Together with the relatively modest sample size, these factors likely contributed to the limited replication of previously reported associations.

Collectively, these findings support an increasingly recognized view that obesity is genetically and biologically heterogeneous [30, 31]. The observed phenotype-selective association patterns suggest that different genetic pathways may preferentially influence overall body mass, body composition, and fat distribution. Integrating adiposity phenotypes beyond BMI, together with emerging biological frameworks such as organokine-mediated inter-organ communication, may therefore improve our understanding of obesity heterogeneity and help identify mechanistically distinct obesity subtypes. Future studies integrating genomic, transcriptomic, proteomic, and circulating organokine data in larger and ethnically diverse populations may provide deeper insight into the biological mechanisms linking genetic variation with individual differences in adiposity phenotypes.

Strengths and Limitations. This study has several strengths First, it integrated two conceptually distinct sources of biological information, namely classical obesity-susceptibility loci and organokine pathway genes, within a unified analytical framework. Second, five complementary adiposity phenotypes were analyzed simultaneously, allowing direct comparison of genetic effects across overall body mass, body composition, and fat distribution measures. Third, rigorous quality-control procedures, linkage disequilibrium assessment, minor allele frequency filtering, and correction for multiple testing were applied to minimize false-positive and unstable findings. Fourth, the study addressed an important gap in the literature by incorporating organokine-related genetic variation into obesity characterization, an area that has received substantially less attention than traditional obesity-susceptibility loci despite growing interest in endocrine communication between adipose tissue, skeletal muscle, liver, and other metabolically active organs.

Several limitations should also be acknowledged. First, the sample size (n = 133) was modest for genetic association analysis. Although the candidate-variant strategy substantially reduced the multiple-testing burden compared with genome-wide approaches, statistical power

608 remained limited, particularly for the comparison of phenotype-specificity patterns and for the
609 detection of modest genetic effects. Second, the cross-sectional design precludes causal
610 inference and does not allow assessment of temporal relationships between genetic variation
611 and adiposity-related phenotypes. Third, the literature-derived obesity-susceptibility and
612 organokine-pathway variant sets may not comprehensively capture all relevant obesity-related
613 loci, and genotyping-array coverage limited the number of published variants available for
614 analysis. Fourth, the study population consisted exclusively of Lithuanian adults with
615 overweight or obesity, potentially limiting the generalizability of the findings to other
616 populations and ancestries. Finally, several of the strongest associations reflected clusters of
617 correlated variants within the same linkage disequilibrium block rather than fully independent
618 association signals. Consequently, the identified loci should be interpreted at the regional
619 rather than individual-variant level until confirmed by fine-mapping studies and independent
620 replication.
621
622 **CONCLUSIONS**
623 This study demonstrates that adiposity-related genetic associations are phenotype-
624 dependent and supports the existence of partially distinct genetic architectures underlying
625 overall body mass, fat distribution, and body composition in metabolically healthy adults with
626 overweight or obesity. While *IL6* emerged as the only locus remaining significant after
627 multiple-testing correction, several additional candidate genes showed phenotype-specific
628 association patterns, highlighting the biological heterogeneity of adiposity. Organokine-
629 pathway variants exhibited a tendency toward broader phenotypic involvement than classical
630 obesity-susceptibility variants, suggesting a potential role for inter-organ signaling pathways
631 in shaping adiposity phenotypes. Collectively, these findings demonstrate that evaluating
632 multiple adiposity measures beyond BMI can reveal biologically distinct genetic signals and

provide a more comprehensive understanding of obesity heterogeneity. Replication in larger independent cohorts and functional characterization of the identified loci, particularly *LDHA*, are warranted.

DECLARATIONS

Ethics declaration / Ethics approval: The study was conducted in accordance with the Declaration of Helsinki. The study protocol was approved by the Vilnius Regional Biomedical Research Ethics Committee (Vilniaus regioninis biomedicininių tyrimų etikos komitetas), Approval No. 2021/11-1393-866.

Consent to Participate declaration: Written informed consent to participate was obtained from all individual participants prior to their inclusion in the study.

Consent to Publish declaration: Not applicable. The manuscript does not contain any individual person's data in any form (including individual details, images or videos).

Data Availability: The individual-level genotype and phenotype data supporting the findings of this study are not publicly available because they contain sensitive personal and genetic information, and participants' consent and the ethics approval (Vilnius Regional Biomedical Research Ethics Committee, Approval No. 2021/11-1393-866) restrict data sharing. The data are available from the corresponding author upon reasonable request and with the permission of the Vilnius Regional Biomedical Research Ethics Committee. The literature-derived candidate variants were obtained from the publicly available GWAS Catalog (https://www.ebi.ac.uk/gwas/home).

Funding Declaration: This research was funded by the Translational Health Research Institute, Faculty of Medicine, Vilnius University. The funder had no role in study design, data collection and analysis, decision to publish, or preparation of the manuscript.

Competing Interest declaration: The authors declare no competing interests.

Author Contribution declaration: A.L. and V.G. conceived and designed the study and developed the methodology. A.L. collected and analysed the data. A.L. and V.G. interpreted the data and wrote the first draft of the manuscript. All authors critically revised the manuscript and read and approved the final version.

Acknowledgements: The authors thank the Population Genomics Group at the Faculty of Medicine, Vilnius University, particularly A. Urnikytė, L. Pranckėnienė and G.Vytė, for their assistance with genotyping procedures. We also express our sincere gratitude to all participants who agreed to take part in this study.

REFERENCES

1. Lotta LA, Wittemans LBL, Zuber V, Stewart ID, Sharp SJ, Luan J, et al. Association of genetic variants related to gluteofemoral vs abdominal fat distribution with type 2 diabetes, coronary disease, and cardiovascular risk factors. JAMA. 2018;320(24):2553-63. doi:10.1001/jama.2018.19329

2. Mouchti S, Orliacq J, Reeves G, Chen Z. Assessment of correlation between conventional anthropometric and imaging-derived measures of body fat composition: a systematic literature review and meta-analysis of observational studies. BMC Med Imaging. 2023;23:127. doi:10.1186/s12880-023-01063-w

3. Agrawal S, Klarqvist M, Diamant N, Stanley T, Ellinor PT, Mehta N, et al. BMI-adjusted adipose tissue volumes exhibit depot-specific and divergent associations with cardiometabolic diseases. Nat Commun. 2023;14. doi:10.1038/s41467-022-35704-5

4. Huang B, DePaolo J, Judy R, Shakt G, Witschey W, Levin M, et al. Relationships between body fat distribution and metabolic syndrome traits and outcomes: a mendelian randomization study. PLoS One. 2023;18. doi:10.1371/journal.pone.0293017

5. Elffers TW, de Mutsert R, Lamb HJ, de Roos A, Willems van Dijk K, Rosendaal FR, et al. Body fat distribution, in particular visceral fat, is associated with cardiometabolic risk factors in obese women. PLoS One. 2017;12. doi:10.1371/journal.pone.0185403

6. Lee V, Han Y, Toh D, Bryant J, Boubertakh R, Le TT, et al. Differential association of abdominal, liver, and epicardial adiposity with anthropometry, diabetes, and cardiac remodeling in Asians. Front Endocrinol (Lausanne). 2024;15. doi:10.3389/fendo.2024.1439691

7. Thomas EL, Frost G, Taylor-Robinson SD, Bell JD. Excess body fat in obese and normal-weight subjects. Nutr Res Rev. 2012;25(1):150-61. doi:10.1017/s0954422412000054

8. Lin B, Hu Y, He H, Chen X, Ou Q, Liu Y, et al. Regional adipose distribution and metabolically unhealthy phenotype in Chinese adults: evidence from China National Health Survey. Environ Health Prev Med. 2025;30. doi:10.1265/ehpm.24-00154

9. Szeliga A, Chedraui P, Męczekalski B. The impact of the menopausal transition on body composition and abdominal fat redistribution. J Clin Med. 2026;15. doi:10.3390/jcm15020740

10. Choi K. The impact of organokines on insulin resistance, inflammation, and atherosclerosis. Endocrinol Metab (Seoul). 2016;31(1):1-6. doi:10.3803/enm.2016.31.1.1

11. Ren Y, Zhao H, Yin C, Lan X, Wu L, Du X, et al. Adipokines, hepatokines and myokines: focus on their role and molecular mechanisms in adipose tissue inflammation. Front Endocrinol (Lausanne). 2022;13. doi:10.3389/fendo.2022.873699

12. Lim JY, Kim E. The role of organokines in obesity and type 2 diabetes and their functions as molecular transducers of nutrition and exercise. Metabolites. 2023;13. doi:10.3390/metabo13090979

13. Letukienė A, Hendrixson V, Ginevičienė V. Current knowledge and scientific trends in myokines and exercise research in the context of obesity. Front Med (Lausanne). 2024;11. doi:10.3389/fmed.2024.1421962

14. Castillo-Armengol J, Fajas L, Lopez-Mejia IC. Inter-organ communication: a gatekeeper for metabolic health. EMBO Rep. 2019;20(9):e47903. doi:10.15252/embr.201947903

15. Priest C, Tontonoz P. Inter-organ cross-talk in metabolic syndrome. Nat Metab. 2019;1:1177-88.

16. Katagiri H. Inter-organ communication involved in metabolic regulation at the whole-body level. Inflamm Regen. 2023;43:60. doi:10.1186/s41232-023-00306-1

17. Ni YQ, Zhan J, Liu YS. Decoding the multiple identities and crosstalk of organokines in obesity-related type 2 diabetes mellitus. Aging Dis. 2025;17(1):5-17. doi:10.14336/ad.2024.1138
18. Pelczyńska M, Miller-Kasprzak E, Piątkowski M, Mazurek R, Klause M, Suchecka A, et al. The role of adipokines and myokines in the pathogenesis of different obesity phenotypes—new perspectives. Antioxidants (Basel). 2023;12. doi:10.3390/antiox12122046
19. Eghbali M, Iranmanesh M, Hatami N, Mobaderi T, Ghadikolaei OA, Cheraghi S. Impact of fat mass and obesity-associated (FTO) gene variants on adult obesity and overweight: a comprehensive meta-analysis. BMC Endocr Disord. 2026;26. doi:10.1186/s12902-026-02209-x
20. Mahmoud R, Kimonis V, Butler MG. Genetics of obesity in humans: a clinical review. Int J Mol Sci. 2022;23. doi:10.3390/ijms231911005
21. Bouchard C. Genetics of obesity: what we have learned over decades of research. Obesity (Silver Spring). 2021;29(5):802-20. doi:10.1002/oby.23116
22. Saqlain M, Khalid M, Fiaz M, Saeed S, Fatima T, Maglio C, et al. Risk variants of obesity associated genes demonstrate BMI raising effect in a large cohort. PLoS One. 2022;17. doi:10.1371/journal.pone.0274904
23. Tan LJ, Zhu H, He H, Wu K, Li J, Chen XD, et al. Replication of 6 obesity genes in a meta-analysis of genome-wide association studies from diverse ancestries. PLoS One. 2014;9. doi:10.1371/journal.pone.0096149
24. Veerabathiran R, Sivakumar S, Kalarani IB, Mohammed V. A review of genes associated with obesity susceptibility: findings from association studies. J Health Sci Med Res. 2023. doi:10.31584/jhsmr.2023959

740 25. Gupta A, Singh AK, Gupta P, Gupta V, Ojha A. Association of adiponectin gene variants
741 (+45T>G and +276G>T) with adipokine levels and metabolic syndrome in North Indian
742 adult women. Diabetes Technol Obes Med. 2025;1. doi:10.1089/dtom.2025.0014
743 26. Nair JM, Chauhan G, Prasad G, Chakraborty S, Bandesh K, Giri AK, et al. Novel genetic
744 associations with childhood adipocytokines in Indian adolescents. Cytokine.
745 2025;190:156935. doi:10.1016/j.cyto.2025.156935
746 27. Staiger H, Böhm A, Scheler M, Berti L, Machann J, Schick F, et al. Common genetic
747 variation in the human FNDC5 locus, encoding the novel muscle-derived 'browning' factor
748 irisin, determines insulin sensitivity. PLoS One. 2013;8.
749 doi:10.1371/journal.pone.0061903
750 28. Humińska-Lisowska K, Bıçakçı B, Michałowska-Sawczyn M, Aschenbrenner P,
751 September A, Proia P, et al. Cytokine gene variants are associated with aerobic fitness-
752 related, hematological, and metabolic traits in healthy adults. Compr Physiol. 2026;16.
753 doi:10.1002/cph4.70234
754 29. Lim SY, Chan YM, Ramachandran V, Shariff ZM, Chin YS, Arumugam M. Dietary acid
755 load and its interaction with IGF1 (rs35767 and rs7136446) and IL6 (rs1800796)
756 polymorphisms on metabolic traits among postmenopausal women. Nutrients. 2021;13.
757 doi:10.3390/nu13072161
758 30. Han MS, White A, Perry RJ, Camporez JP, Hidalgo J, Shulman GI, et al. Regulation of
759 adipose tissue inflammation by interleukin 6. Proc Natl Acad Sci U S A. 2020;117(6):2751-
760 60. doi:10.1073/pnas.1920004117
761 31. Claussnitzer M, Dankel SN, Kim KH, Quon G, Meuleman W, Haugen C, et al. FTO obesity
762 variant circuitry and adipocyte browning in humans. N Engl J Med. 2015;373(10):895-907.
763 doi:10.1056/nejmoa1502214

764 32. Rubinstein M, Low MJ. Molecular and functional genetics of the proopiomelanocortin
765 gene, food intake regulation and obesity. FEBS Lett. 2017;591(17):2593-606.
766 doi:10.1002/1873-3468.12776
767 33. Kos K, Wilding JP. SPARC: a key player in the pathologies associated with obesity and
768 diabetes. Nat Rev Endocrinol. 2010;6(4):225-35. doi:10.1038/nrendo.2010.18
769 34. Eder K, Baffy N, Falus A, Fulop AK. The major inflammatory mediator interleukin-6 and
770 obesity. Inflamm Res. 2009;58(11):727-36. doi:10.1007/s00011-009-0060-4
771 35. Sindhu S, Thomas R, Shihab P, Sriraman D, Behbehani K, Ahmad R. Obesity is a positive
772 modulator of IL-6R and IL-6 expression in the subcutaneous adipose tissue: significance
773 for metabolic inflammation. PLoS One. 2015;10(7):e0133494.
774 doi:10.1371/journal.pone.0133494
775 36. Brooks GA. Lactate as a fulcrum of metabolism. Redox Biol. 2020;35:101454.
776 doi:10.1016/j.redox.2020.101454
777 37. Lindberg I, Fricker LD. Obesity, POMC, and POMC-processing enzymes: surprising
778 results from animal models. Endocrinology. 2021;162(12):bqab155.
779 doi:10.1210/endocr/bqab155
780 38. Nie J, Sage EH. SPARC functions as an inhibitor of adipogenesis. J Cell Commun Signal.
781 2009;3(3-4):247-54. doi:10.1007/s12079-009-0064-4
782 39. Ruiz-Ojeda FJ, Méndez-Gutiérrez A, Aguilera CM, Plaza-Díaz J. Extracellular matrix
783 remodeling of adipose tissue in obesity and metabolic diseases. Int J Mol Sci.
784 2019;20(19):4888. doi:10.3390/ijms20194888